Reproductive Biology 20 (2020) 37–41

Contents lists available at ScienceDirect

Reproductive Biology

journal homepage: www.elsevier.com/locate/repbio

Original article

Shape and size of epididymal sperm from Gir bulls using atomic force microscopy: A nanoscale characterization of epididymal sperm

Andrielle Thainar Mendes Cunha[a], Luciano Paulino Silva[b], José Oliveira Carvalho[c], Margot Alves Nunes Dode[b,*]

[a] Institute of Biology, University of Brasília, Brasília, Brazil
[b] Embrapa Genetic Resources and Biotechnology, Brasília, Brazil
[c] Veterinary Medicine Department, University of Espírito Santo, Alegre, Brazil

ARTICLE INFO

Keywords:
Sperm head
Cattle
Morphology
Biotechnology

ABSTRACT

As epididymal sperm (EP) are not exposed to seminal plasma, they are physiologically different from ejaculated spermatozoa (EJ). Therefore, the aim of this study was to morphologically characterize the head of EP recovered from the epididymis tail, and to evaluate if the physiological differences between EP and EJ were also expressed in the head's shape and size. EP and EJ were recovered from seven Gir bulls and were individually assessed. Sperm cells were washed, fixed, and 20 cells from each animal were analyzed by atomic force microscopy (AFM). The images were acquired through contact mode. Then, an off-line processing software was used and the images acquired were manually segmented using digital zoom of the original images. Twenty-four structural features were assessed including one, two, and three dimensional parameters, and also shape descriptors which were calculated based on the one and two dimensional parameters. Data were compared by *t*-test, then, a collective analysis was performed using principal component analysis (PCA). The EP group presented higher roughness and elongation ($P \leq 0.05$), and smaller form factor and circularity rate than that of the EJ group ($P \leq 0.05$). For the other parameters no differences ($P \geq 0.05$) were observed. In addition, in the PCA analysis no differences among EP and EJ were observed either ($P \leq 0.05$). This study showed that EP and EJ collected from the same sire presented similar characteristics in nineteen of the twenty-four parameters evaluated, indicating that absence of seminal plasma does not affect the morphology of EP.

1. Introduction

When sperm cells leave the testes, they are not yet able to fertilize an oocyte, since they need to undergo two important extra-testicular processes; maturation and capacitation. As soon as they are released in the lumen of the seminiferous tubules of the testis, they are transported to the epididymis. During their transit in the epididymis, sperm undergo maturation process, which is characterized by both morphological and physiological modifications that are necessary for them to acquire fertility. These modifications include changes in the biochemical profiles of sperm membrane, final condensation of chromatin, transit of the cytoplasmic droplets, and acquisition of progressive motility [1–3].

After sperm transit through the epididymis, matured sperm are stored in the epididymis tail until ejaculation, when are mixed with seminal plasma. At this time, spermatozoa are coated in a series of molecules including heparin binding proteins family called "Binder Sperm Proteins" (BSPs). This coating is responsible for important events such as the stability of the plasma membrane, formation of sperm reservoirs, formation of membrane specific sites for heparin binding, capacitation, and sperm binding to the zona pellucida [4–8].

Since epididymal sperm (EP) are not exposed to seminal plasma, they are physiologically different from the ejaculated spermatozoa (EJ) [8,9]. In fact, the physiological differences between EP and EJ regarding resistance to refrigeration, post-thaw longevity, and binding to isthmus cells have already been demonstrated [10]. More recent findings using in vitro assays suggest that EP are responsive to heparin supplementation [9], and require less time for in vitro capacitation [9,11] than EJ sperm. All of these physiological differences lead us to hypothesize that the morphology of EP could also be different to EJ sperm.

This question was also raised by another study using Iberian red deer [12]; however, this study used conventional light microscopy. Most of the reports that study the characterization of EJ sperm use

* Corresponding author.
E-mail address: margot.dode@embrapa.br (M.A.N. Dode).

https://doi.org/10.1016/j.repbio.2019.12.007
Received 21 September 2019; Received in revised form 17 December 2019; Accepted 22 December 2019
Available online 31 December 2019
1642-431X/

protocols that include dyes, and usually the structural dimensions are determined manually, which may not detect possible differences. In fact, studying rabbit spermatozoa, Ierardi et al. [13] showed that the precise details of the spermatozoa structure could not be detected by manual methods that offer limited resolution. One alternative to evaluate the morphology more accurately is to use atomic force microscopy (AFM) technique which represents an effective tool for analyze topographical surfaces of biological or non biological samples with resolution at nanoscale.

This technique has become an invaluable multidisciplinary tool for the advanced characterization of different materials. In its basic application, it provides high-resolution images of surface structures at scales ranging from a few nanometers to hundreds of micrometers [14,15].

AFM-based strategies have been used for studies of the sperm cell such as structural characterization [13], analysis of organization of sperm plasma membrane [15,16], investigation of specific morphological defects [17,18], and interaction of extracellular molecules with membrane proteins [15,19]. However, to our knowledge, no studies have been conducted comparing EJ and EP from the same animal using AFM-based approaches.

Thus, the aim of this study was to use AFM as a tool to morphologically characterize EP and to compare its morphology with EJ sperm of the same sires.

2. Materials and methods

2.1. Chemicals and ethics committee approval

Unless otherwise indicated, all reagents were purchased from Sigma-Aldrich (St. Louis, MO, USA). All procedures with animals were approved by the Ethics Committee of Embrapa's Animal Genetic Resources and Biotechnology (Protocol CEUA–Cenargen 004/2013).

2.2. Animals

Seven Gir bulls (*Bos taurus indicus*) aged between 36 and 40 months were selected and used for EP and EJ sperm recovery. Animals were raised in an extensive system and fed pasture (*Brachiaria brizantha*), with mineral salt and water provided *ad libitum*. Prior to the experiment, the bulls were subjected to three andrological evaluations, and only sires that showed a subjective total sperm motility of at least 70 % and a minimum of 70 % morphologically normal sperm were used for the experiment.

2.3. Sperm collection and cryopreservation

Sperm samples were collected from ejaculate and the epididymal tail of the same animal according to the method described by Cunha et al. [10]. Briefly, one ejaculate was collected via electroejaculation from each Gir bull and seven to fifteen days after semen collection, all sires were orchiectomized.

The testes were cleaned with saline solution (0.9 % NaCl) and 70 % ethanol, and sperm collection from the cauda epididymis was performed [10]. Each epididymis was thoroughly cleaned and the superficial blood vessels of the tail were punctured so that most of the blood could be removed. Next, the sperm from the epididymis tail were collected by a series of cuts.

After recovery, the EJ or EP spermatozoa were diluted in Tris-citrate-yolk-glycerol Dilutris extender (SEMENCON–Agricultural Products Ltd., Porto Alegre, RS, Brazil), loaded at a concentration of 25–30 $\times$ 10^6 sperm/straw (0.25 mL) and cryopreserved.

2.4. Sperm processing for analysis

One straw of each animal from each group (EP and EJ) was thawed at 37 °C. After thawing, one aliquot of 20 μL from each animal sample was removed for acrosome integrity assessments and the remaining was processed to AFM analyses according to Carvalho et al. [20]. Briefly, each sperm sample was centrifuged for 5 min at 200 $\times$ *g* to remove the extender. The supernatant containing the extender was discarded and the pellet was fixed for 5 min in 1 mL of formaldehyde saline (1.6 %) and then centrifuged for 5 min at 200 $\times$ *g*.

After centrifugation, the supernatant was discarded and the pellet was washed by centrifugation twice in 1 mL of ultrapure water for 5 min at 200 $\times$ *g*. Finally, the pellet was resuspended in approximately 150 μL of ultrapure water and 2 μL of this sample were deposited onto glass coverslips and air dried for AFM assessments.

2.5. Acrosome integrity analysis

Acrosome status was assessed using fluorescein isothiocyanate conjugated with peanut agglutinin (FITC-PNA, Invitrogen, Eugene, USA) and propidium iodide (PI) (Molecular Probes, Eugen, USA) as previously described [9]. The working solution for staining consisted of 100 μL of sodium citrate (3 % diluted in 0.9 % NaCl), 1 μL of PI (0.5 mg/mL), and 1.5 μL of FITC-PNA solution (1 mg/mL in PBS). PI-negative sperm were considered alive, and PI-positive sperm were considered dead. Alive or dead cells were classified as acrosome-reacted (FITC-PNA positive) or as acrosome-intact (FITC-PNA negative).

Assessments were performed by flow cytometry on an AMNIS FlowSight Image Cytometer (Amnis Corp., Seattle, WA) using the INSPIRE V6.1 acquisition software. Fluorescent dyes were excited by lasers at 488 nm at 10 mW and 405 nm at 30 mW. A specific acquisition template was previously created for identifying and acquiring only sperm cells. Thus, 10,000 events were collected per sample/parameter evaluated. For analysis of the results, dot plot graphs were created from unstained control samples, and the populations were gated based on stain patterns.

2.6. Atomic force microscopy analysis

For the AFM analyses (Fig. 1), a SPM-9600 microscope (Shimadzu, Japan) was used and the images were acquired by contact mode [21], using 200 μm length V cantilevers (constant of ~ 0.15 N/m, 24 kHz resonance frequency) with integrated pyramidal tip (radius of curvature < 20 nm). A scanner with a The 100 μm extension was used for scanning travel following the XY direction and 7 μm in the Z direction. The acquisition of the images was performed at 512 $\times$ 512 pixels and a scan rate of 1 Hz.

The images were processed according to Carvalho et al. [20], using SPM-9600 off-line software. The processing consisted of an automatic plane fit leveling the surface. A total of forty individual cells, twenty cells per each group (EP and EJ) were assessment per animal and manually segmented using a digital zoom of the original image whilst using the labeling function of the particle analysis software.

Then, cell measurements were performed on the sperm head. Twenty-four characteristics were assessed, including one, two, and three dimensional measures, and shape descriptors. Shape descriptor values were obtained using a mathematical formula with one and two dimensional values (for details, see mathematical formulas below).

2.7. Mathematical formulas used to generate the shape descriptors

In this study, shape descriptors were calculated using the mathematical formulas described below.

Form factor: (4 $\times$ pi $\times$ Area excluding hole)/ (Perimeter $\times$ Perimeter).

Roundness: (4 $\times$ Area including hole)/pi $\times$ (Maximum diameter $\times$ Maximum diameter).

Aspect ratio: Maximum diameter/Pattern width.

Effective diameter: (Area including hole/pi) $\times$ 2.

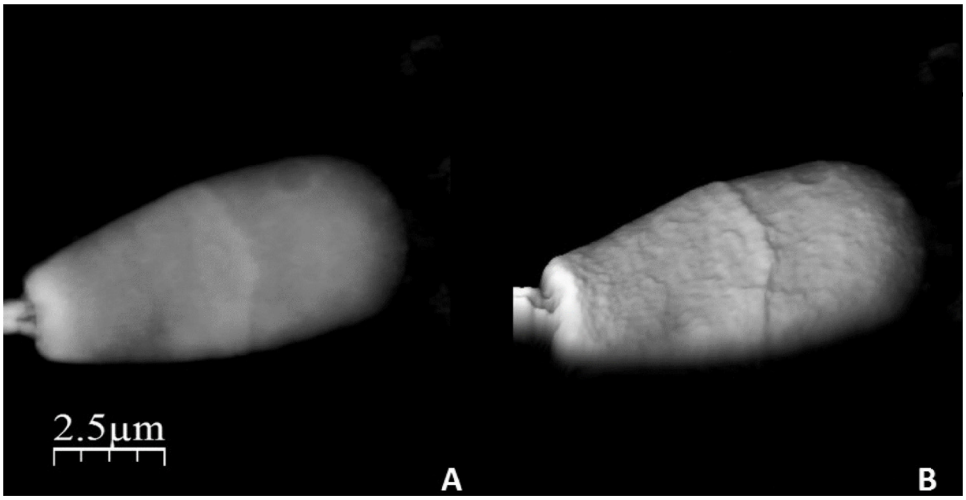

Fig. 1. Atomic force microscopy images of 2D (A) and 3D view (B) of epididymal sperm.

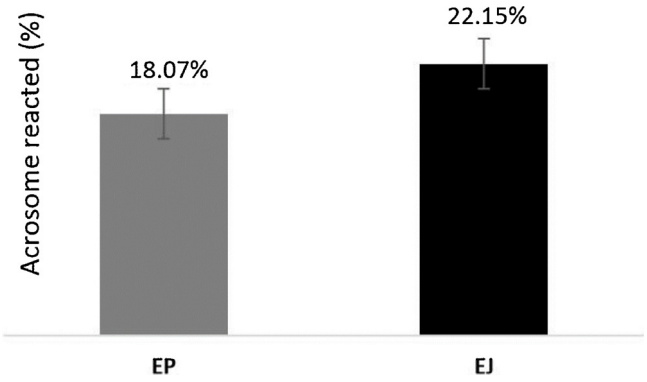

Fig. 2. Percentage of sperm cells with acrosome reacted of bovine spermatozoa (mean obtained from seven sires) recovered from epididymal tail (EP) and ejaculation (EJ). Data analyzed by Tukey test (P ≤ 0.05).

Circular degree: pi × maximum diameter/4 × area excluding hole.

Circularity ratio: (4 × pi × Area including hole)/Perimeter × Perimeter.

Thin degree: maximum diameter/pattern width.

Compact aspect rate: (square root ((4/pi) × Area including hole))/ Maximum diameter.

Elongation: (Perimeter × Perimeter)/Area including hole.

Roughness: (Perimeter × Perimeter)/(4 × pi × area excluding hole).

2.8. Statistical analyses

Data from the means of the twenty-four parameters obtained by AFM and the acrosome assessments and the characters of each animal were compared between the groups (EP and EJ) by *t*-test (P ≤ 0.05). Then, the twenty-four parameters were also collectively evaluated by a principal component analysis (PCA). All data were analyzed by Past3 software and are presented as mean ± standard deviation (SD).

3. Results

To avoid an effect of the absence of acrosome in the sperm head volume, one sample from each animal was removed for the evaluation of the acrosomal integrity. According to Fig. 2, no differences in the percentage of cells with intact acrosomes were detected among the EP (18.07 %) and EJ (22.15 %) groups.

The values for one, two, and three dimensional parameters are depicted in Table 1, which showed no significant differences between the EJ and EP sperm heads. Otherwise, shape descriptors (Table 2) showed that the EP group presented higher roughness and elongation, and smaller form factor and circularity rate than that of the EJ group.

A simultaneous evaluation of all the measured traits was performed using a PCA, to determine if it was possible to distinguish and identify to which group belong the cells of each individual.

The results are showed in Fig. 3, in which both groups are represented by just one cluster, containing dots of different colors. Meaning that the EP and EJ groups can not be distinguished from each

Table 1
One, two, and three dimensional values (± SD) of bovine sperm recovered from epididymal (EP) and ejaculated (EJ) sources, as evaluated by atomic force microscopy.

Measures of structural characteristics one dimensional

Groups	Mean Radius (µm)	Mean Radius Variance (µm)	Maximum Z (µm)	Minimum Z (µm)	Average Z (µm)	Maximum Diameter (µm)	Pattern Width (µm)
EP	4.14 ± 0.13	1.11 ± 0.08	0.48 ± 0.05	0.16 ± 0.02	0.29 ± 0.04	11.69 ± 0.4	7.69 ± 0.58
EJ	4.21 ± 0.14	1.13 ± 0.06	0.52 ± 0.03	0.16 ± 0.02	0.31 ± 0.04	12.13 ± 0.49	9.32 ± 1.11

Measures of structural characteristics two and three dimensional

Groups	Perimeter (µm)	C Perimeter (µm)	Area including hole (µm^2)	Surface area (µm^2)	Volume (µm^3)
EJ	30.9 ± 1.2	28.4 ± 1.3	49.6 ± 2.9	50.4 ± 2.9	15.9 ± 2.2
EP	31.1 ± 1.3	28.2 ± 1.0	47.9 ± 3.2	48.8 ± 3.4	15.6 ± 2.3

Values are a mean ± of 140 sperm cells for each group.
No difference were observed (P > 0.05).

Table 2
Shape descriptor parameters (± SD) of the bovine epididymal (EP) and ejaculate (EJ) sperm evaluated by atomic force microscopy.

Group	Distortion	Circular Degree	Roughness	Thin Degree	Form Factor	Roundness	Aspect Ratio	Effective diameter	Circularity ratio	Compact aspect rate	Elongation	Degree of circularity
EJ	0.72 ± 0.05	2.27 ± 0.13	1.62 ± 0.07[a]	1.65 ± 0.15	0.62 ± 0.03[a]	0.45 ± 0.02	1.53 ± 0.13	7.81 ± 0.26	0.62 ± 0.03[a]	0.67 ± 0.02	20.24 ± 0.85[a]	0.79 ± 0.02
EP	0.74 ± 0.05	2.26 ± 0.09	1.54 ± 0.06[b]	1.60 ± 0.17	0.65 ± 0.03[b]	0.45 ± 0.02	1.46 ± 0.17	7.94 ± 0.23	0.65 ± 0.03[b]	0.67 ± 0.01	19.23 ± 0.72[b]	0.81 ± 0.02

Values are an average of 140 sperm cells for each group.
[a,b] Within each column indicate significant differences between EP and EJ groups as analyzed by a Tukey test ($P \leq 0.05$).

other.

4. Discussion

The use of EP in reproductive biotechnology represents an alternative for the storage and use of gametes recovered from individuals with acquired fertility problems or that die suddenly. Although there are physiological differences between EP and EJ sperm, such as capacitation process and longevity [9,11], EP can fertilize an oocyte as efficiently as EJ sperm.

The differences in physiological behavior, mainly due to not being exposed to seminal plasma, could lead to morphological differences such as dimensions or shape of the sperm head. These characteristics are not perceptible in routine evaluations using conventional light microscopy [12,22], and may be detected using other techniques. AFM is able to detect differences between the size and shape of various biological molecules, such as proteins and extracellular molecules that adhere to the membrane [15,19,23].

Therefore, to test our hypothesis that EP and EJ, besides being different in their physiological behavior, are also morphological different, we chose to use AFM for the analysis of sperm morphology.

It is well described that the pre-equatorial region of the sperm head with a reacted acrosome is approximately 40 % smaller than that of the spermatozoon with an intact acrosome [16,17]. Therefore, to avoid interference of the acrosomal volume on the total volume of the spermatozoon head between groups, one sample from each animal was evaluated for acrosome integrity. No differences were found between the EP and EJ groups for acrosome integrity.

Regarding to AFM analysis, size and shape of the spermatozoa were similar between the EP and EJ for all parameters observed in one, two, and three dimensional measurements. However, among shape descriptors, roughness and elongation showed higher values, and form factor and circularity rate showed lower values for EP group than for EJ group. In human and bovine sperm, roughness has been correlated with acrosomal reaction [17,24].

However, in the present study the amount of spermatozoa with an acrosome reaction was similar between the EP and EJ groups, and could not explain the difference found between them. It is possible that other characteristics of EP plasma membrane such as the absence of seminal plasma proteins and quantity of cholesterol can also be responsible by these shape descriptors differences. In an attempt to verify if the EP and EJ could be distinguished from each other when various characteristics are simultaneously taken into account, a PCA was performed. According to our results, PCA analysis failed in discriminating groups of sperm.

In a previous study from our group using sexed sperm [20], differences in some shape descriptors were also observed. However, in that study, it was possible to differentiate sperm cell carrying X from those carrying Y chromosome by multivariate analysis. In contrast, in the present even though there were difference in some shape descriptors data between EP and EJ, these differences were not sufficient to differentiate EP from the EJ group.

It is possible that some factors involved in sample preparation could have contributed to this lack of difference. One example is the washing steps for coverslip preparations that could remove or cleave the structures present in the EJ membrane. In addition to the washing process, another factor that may have interfered with the results is cryopreservation. Cryopreservation could induce changes in both the EP and EJ, so that when they were thawed, they showed similar characteristics. In fact, the cryopreservation process has already been reported to modify the structure of the molecules that are anchored to the membrane [25], as well as decrease sperm dimensions [12,22].

On the other hand, we used the same animals as the donors of EP and EJ, avoiding variation among individuals, which allows having greater confidence in the data. Thus, the results showed that the lack of exposure to seminal plasma does not induce a perceptible change on

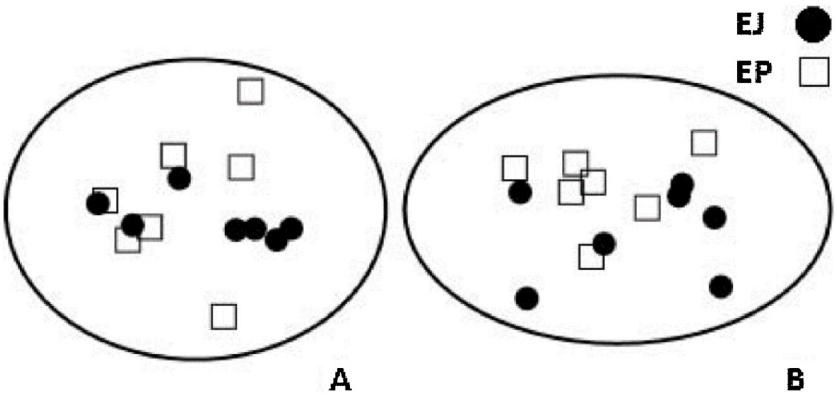

Fig. 3. Principal component analysis of the sperm recovered from the epididymal tail (EP) and ejaculate (EJ) using one two and three dimensional measurements (A) and using shape descriptor parameters (B). Each point represents one bull of each group, from the average of 20 sperm cells per bull, to a total of 140 sperm cells for each group.

overall sperm morphology. This knowledge about EP morphology assessed by a tool that can identify even nanostructures can have an important application in the field of studies regarding EP and epididymis biology.

Based on the obtained results, it is possible to confirm that sperm recoveries from EP are morphologically similar to EJ in most of the aspects evaluated, indicating that absence of seminal plasma does not affect the morphology of EP.

Funding

Brazilian agriculture research company, Brazilian National Council for Scientific, University of Brasilia – UnB and Technological Development (CNPq), supported this work. The funders had no role in study design, data collection and analysis, decision to publish, or preparation of the manuscript.

Declaration of Competing Interest

The author affirm that this study don't have conflict of interest.

References

[1] Cornwall GA. New insights into epididymal biology and function. Hum Reprod Update 2009;15:213–27.
[2] Dacheux JL, Dacheux F. New insights into epididymal function in relation to sperm maturation. Reproduction 2014;147:R27–42.
[3] Gervasi MG, Visconti PE. Molecular changes and signaling events occurring in spermatozoa during epididymal maturation. Andrology 2017;5:204–18.
[4] Miller DJ, Winer MA, Ax RL. Heparin-binding proteins from seminal plasma bind to bovine spermatozoa and modulate capacitation by heparin. Biol Reprod 1990:42.
[5] Thérien I, Moreau R, Manjunath P. Major proteins of bovine seminal plasma and high-density lipoprotein induce cholesterol efflux from epididymal sperm. Biol Reprod 1998;59:768–76.
[6] Manjunath P, Thérien I. Role of seminal plasma phospholipid-binding proteins in sperm membrane lipid modification that occurs during capacitation. J Reprod Immunol 2002;53:109–19.
[7] Gwathmey TM, Ignotz GG, Mueller JL, Manjunath P, Suarez SS. Bovine seminal plasma proteins PDC-109, BSP-A3, and BSP-30-kDa share functional roles in storing sperm in the oviduct. Biol Reprod 2006;75:501–7.
[8] Rodriguez-Villamil P, Hoyos-Marulanda V, Martins JA, Oliveira AN, Aguiar LH, Moreno FB, et al. Purification of binder of sperm protein 1 (BSP1) and its effects on bovine in vitro embryo development after fertilization with ejaculated and epididymal sperm. Theriogenology 2016;85:540–54.
[9] Cunha ATM, Carvalho JO, Guimaraes ALS, Leme LO, Caixeta FM, Viana JHM, et al. Bovine epididymal spermatozoa treatment for in vitro fertilization: heparin accelerates fertilization and enables a reduction in coincubation time. PLoS One 2019;14:e0209692.
[10] Cunha ATM, Carvalho JO, Kussano NR, Martins CF, Mourao GB, Dode MAN. Bovine epididymal spermatozoa: resistance to cryopreservation and binding ability to oviductal cells. Cryobiology 2016;73:348–55.
[11] Matas C, Sansegundo M, Ruiz S, Garcia-Vazquez FA, Gadea J, Romar R, et al. Sperm treatment affects capacitation parameters and penetration ability of ejaculated and epididymal boar spermatozoa. Theriogenology 2010;74:1327–40.
[12] Esteso MC, Fernández-Santos MR, Soler AJ, Montoro V, Quintero-Moreno A, Garde JJ. The effects of cryopreservation on the morphometric dimensions of Iberian red deer (Cervus elaphus hispanicus) epididymal sperm heads. Reprod Domest Anim 2006;41:241–6.
[13] Ierardi V, Niccolini A, Alderighi M, Gazzano A, Martelli F, Solaro R. AFM characterization of rabbit spermatozoa. Microsc Res Tech 2008;71:529–35.
[14] Silva LP. Imaging proteins with atomic force microscopy: an overview. Curr Protein Pept Sci 2005;6:387–95.
[15] Whited AM, Park PS. Atomic force microscopy: a multifaceted tool to study membrane proteins and their interactions with ligands. Biochim Biophys Acta 2014;1838:56–68.
[16] Jones R, James PS, Howes L, Bruckbauer A, Klenerman D. Supramolecular organization of the sperm plasma membrane during maturation and capacitation. Asian J Androl 2007;9:438–44.
[17] Saeki K, Sumitomo N, Nagata Y, Kato N, Hosoi Y, Matsumoto K, et al. Fine surface structure of bovine acrosome-intact and reacted spermatozoa observed by atomic force microscopy. J Reprod Dev 2005;51:293–8.
[18] Ma Y, Xie N, Li Y, Zhang B, Xie D, Zhang W, et al. Teratozoospermia with amorphous sperm head associate with abnormal chromatin condensation in a Chinese family. Syst Biol Reprod Med 2018:1–10.
[19] Barboza JM, Medina H, Doria M, Rivero L, Hernandez L, Josh NV. Use of atomic force microscopy to reveal sperm ultrastructure in HIV patients on highly active antiretroviral therapy. Arch Androl 2004;50:121–9.
[20] Carvalho JO, Silva LP, Sartori R, Dode MAN. Nanoscale differences in the shape and size of X and Y chromosome-bearing bovine sperm heads assessed by atomic force microscopy. PLoS One 2013;8:e59387.
[21] Bonatto CC, Magalhães BS, Branco JO, Durigon EL, Silva LP. Shape and size of red blood cells from the Pygoscelid penguins of Antarctica using atomic force microscopy. Polar Biol 2008;32:287–93.
[22] Esteso MC, Fernández-Santos MR, Soler AJ. J. GJ. Head dimensions of cryopreserved red deer spermatozoa are affected by thawing procedure. CryoLetters 2003;24:261–8.
[23] Gonçalves RP. Atomic force microscopy imaging of membrane proteins. Acta Physica Polonica 2010;117:18–23.
[24] Kumar S, Chaudhury K, Sen P, Guha SK. Quantitative analysis of surface microroughness alterations in human spermatozoa using atomic force microscopy. J Microsc 2007;227:118–23.
[25] Ardon F, Suarez SS. Cryopreservation increases coating of bull sperm by seminal plasma binder of sperm proteins BSP1, BSP3, and BSP5. Reproduction 2013;146:111–7.